Macromolecules

pubs.acs.org/Macromolecules Article

Effect of Coordination Sacrificial Bond Strength on Toughening Properties of Polyesters

Jie Chen, Sheng Wang, Jie Huan, Zhikai Li, Xiaoming Yang, Xiaohong Li,* and Yingfeng Tu*

Cite This: *Macromolecules* 2024, 57, 4054−4061 Read Online

ACCESS | Metrics & More | Article Recommendations | Supporting Information

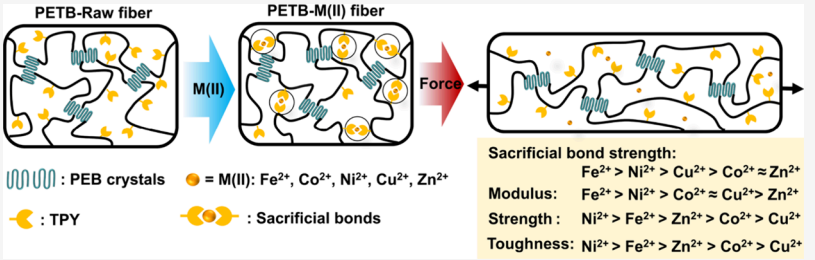

ABSTRACT: By the coordination of dangling terpyridine (TPY) ligands with transition metal ions to form supramolecular cross-linking points as sacrificial bonds (SBs), a double-cross-linked system is constructed from the physically cross-linked semicrystalline polyesters. The mechanical properties are greatly enhanced, and the effect of coordination interaction strength on the toughening effect has been investigated by using different ions (Fe^{2+}, Co^{2+}, Ni^{2+}, Cu^{2+}, and Zn^{2+}). It shows that stronger coordination bonds provide a larger Young's modulus, but not for strength and toughness, which increase first and then decrease after achieving a maximum value at an optimal SB strength. This is due to the properties estimated at different strains, where the supramolecular and physically cross-linking points behave differently. Our results demonstrate that SB strength is not the higher, the better, which should be useful for the design of strong and tough materials.

INTRODUCTION

Inspired by *Nature*, where spider silks and mussel byssus are strong and tough materials, introducing weak interactions into a polymeric material can greatly improve its mechanical properties.[1−3] These weak interactions are defined as sacrificial bonds (SBs) since they are broken preferentially before covalent bonds, following the energy dissipation mechanism and releasing the hidden length of chains.[4−7] To now, a variety of weak bonds (interactions), including hydrogen bonds,[8−10] metal−ligand coordination bonds,[11−16] and ionic interactions,[17,18] have been utilized to be incorporated into polymers with good toughening effect. Among them, due to the available abundance of metal ions and ligands, the metal−ligand coordination bonds have attracted great research interests.[19−22] For example, by the incorporation of pyridine−Zn^{2+} coordination bonds into butadiene−styrene−vinylpyridine vulcanizing rubber, the modulus, strength, and toughness increased several times without sacrificing the extensibility.[23] Other metal−ligands coordination interactions, including pyrimidinone−Zn^{2+}, bipyridine−Zn^{2+}, terpyridine−Fe^{2+}, and catechol−Fe^{3+} interactions, have also been reported for the toughening of elastomers.[23−25]

To now, most of the reported research works have focused on the toughening effect by studying the property differences after the introduction of SBs.[26−30] Since the energy required to break the weak bonds is varied for different SBs, the SB strength should also affect the properties of elastomers. The difficulty lies in the design of a system where other effects are similar while only the SB strength is different. This is hard to be achieved in most systems but is feasible when using metal-coordination interactions as SBs since the strength of coordination bonds can be flexibly tuned by varying the metal ions.[31−34] However, the interactions of pyridine-type ligands with transition metals are usually very weak; thus, their effects on the properties of elastomers are hard to be investigated. Compared to mono- and bidentate ligands, tridentate ligands exhibit a much larger binding affinity range due to the efficient chelation. For example, terpyridine (TPY) can coordinate with a variety of transition metal ions to form $M(TPY)_2^{2+}$, with the binding constant varying from $10^{4.4}$ M^{-1} for Mn^{2+} to $10^{10.7}$ M^{-1} for Ni^{2+}.[35]

In this work, we demonstrate a strategy to construct a toughening system where only the SBs are different. Polyesters with dangling TPY ligands were synthesized via a cascade polycondensation-coupling ring-opening polymerization

Received: November 29, 2023
Revised: March 4, 2024
Accepted: April 8, 2024
Published: April 16, 2024

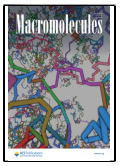

https://doi.org/10.1021/acs.macromol.3c02452
Macromolecules 2024, 57, 4054−4061

Scheme 1. Schematic Illustration of the Synthesis of PETB Copolyesters via PROP

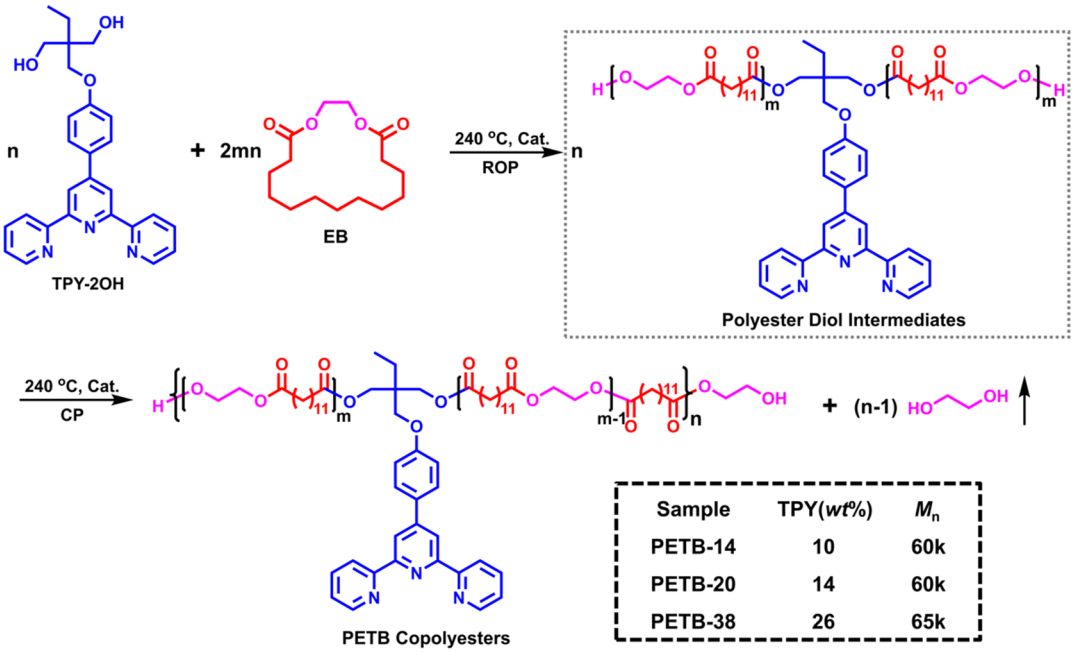

ROP: Ring-Opening Polymerization; CP: Condensation Polymerization

(PROP) method,[36−39] and the SBs were introduced for toughening by the complexation of TPY with transition metal ions, as shown in Scheme 1. Since Fe^{2+}, Co^{2+}, Ni^{2+}, Cu^{2+}, and Zn^{2+} are frequently used first-row transition metal ions that form coordination complex with TPY with different binding energy,[40] the strength of metal−ligand coordination interactions was thus adjustable where Fe^{2+} has the strongest while Zn^{2+} has the weakest. The properties of toughened elastomers were studied to reveal the effect of the introduced coordination bonds on the material properties. It should be noted that Cu^{2+} ions (and Zn^{2+} slightly) can form monocoordination complexes with TPY when used in excess[40]; thus, their behavior may be different from that of those ions forming stable $M(TPY)_2^{2+}$ dicoordination complexes.

RESULTS AND DISCUSSION

The dihydroxyl-terminated TPY (TPY-2OH) initiator was synthesized via Kröhnke-type condensation reaction of 2-acetylpyridine and *p*-chlorobenzaldehyde followed by etherification reaction under the catalysis of calcium hydride (Scheme S1 and Figures S1−S4).[41,42] To investigate the effect of TPY content on properties of toughened elastomers, a series of TPY-containing copolyesters, poly(ethylene-*co*-2-(4-((2,2′:6′,2″-terpyridinyl)-4′-phenoxy)methyl)-2-ethyl-propylene brassylate) (PETB), with various TPY contents were prepared via *in situ* cascade PROP with TPY-2OH and ethylene brassylate (EB) as monomers (Scheme 1). The obtained polymers are coded as PETB-*n*, where *n* donates the average number of TPY per chain evaluated by ^{1}H NMR spectroscopy. The detailed synthetic route and characterization results are provided in the Supporting Information (Figures S5−S6). Gel permeation chromatography (GPC) results confirmed that PETB copolyesters possessed a similar relative number-average molecular weight (M_n) of around 60 kg/mol (Figure S5), while ^{1}H quantitative NMR results provide similar results as summarized in Table 1. The average TPY number in a copolymer chain can be flexibly tailored by the feeding ratio of TPY-2OH and EB, which is ∼38 in PETB-38, and gradually reduced to 14 in PETB-14. All the monomer conversions are over 98%, indicating the efficient atomic utilization of the PROP method.

Table 1. Polymerization Results of PETB Copolyesters

sample	N_{EB} [a]	N_{TPY} [a]	conv.[b] (%)	M_n[c] (kg/mol)	M_n[d] (kg/mol)	$Đ$[e]
PETB-38	186	38	98	64.8	64.2	2.1
PETB-20	195	20	99	60.2	62.1	2.1
PETB-14	204	14	98	60.3	64.2	1.8

[a]Total repeating unit number of TPY (N_{TPY}) and EB (N_{EB}). [b]Conversion of monomer EB. [c]Determined by ^{1}H quantitative NMR. [d]Determined by GPC. [e]Polydispersity determined by GPC.

The PETB copolyesters show good thermal stability with 5% weight loss temperature above 360 °C, from thermogravimetric analysis (Figure S7). Differential scanning calorimetry (DSC, Figure S8) and wide-angle X-ray diffraction (WAXD, Figure S9) measurements indicate poly(ethylene brassylate) (PEB) segments crystallized with melting peaks varied between 58 and 66 °C.[43,44] The melting and crystallization temperatures of PEB segments decrease with the increment of TPY content as well as their crystallinity (Table S1). Interestingly, a significant "negative" peak was observed during the heating curve of PETB-38, which is ascribed to the cold crystallization of the PEB segments. As the TPY segments can be regarded as defects in PEB main chains, the crystallization rate of PEB decreased with the increment of the TPY content. As a result, some of the PEB segments were unable to crystallize during the first cooling process for copolymers with high TPY content. These PEB segments crystallized during the second heating process when the temperatures were higher than the glass transition temperature, leading to the observation of a cold crystallization peak.

https://doi.org/10.1021/acs.macromol.3c02452
Macromolecules 2024, 57, 4054−4061

As the one-dimensional oriented fibrous structure is also critical to achieve high toughness,[25,45] PETB raw fibers were prepared by the melt-spinning of corresponding copolyesters and used to investigate the coordination process with transition metal ions. The diameter of the fibers is 140 ± 10 μm, estimated by optical microscopy (OM, Figure 1a), with

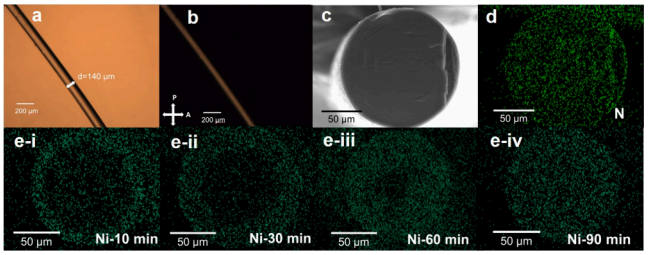

Figure 1. Optical microscopy (a) and polarizing optical microscopy (b) images of PETB-38 fibers; (c) SEM image of cross-section area of the PETB-38-Ni^{2+} fibers with 90 min soaking time; EDS mapping of cross-section area of element N (d) and Ni^{2+} with different soaking times (e: i, 10 min; ii, 30 min; iii, 60 min; iv, 90 min).

strong birefringence observed from polarized optical microscopy (Figure 1b) due to the structure orientation generated during the spinning traction process. The fibers were soaked into 1.0 wt % large excess transition metal salt (Fe^{2+}, Co^{2+}, Ni^{2+}, Cu^{2+}, and Zn^{2+}) methanol solutions for their complexation with TPY ligands, affording toughened fibers with a supramolecular coordination and physical crystallization double-cross-linked structure. Figure 1c shows the scanning electron microscope (SEM) image of the cross-section region of toughened fibers after soaking in 1.0 wt % Ni^{2+} solution for 90 min. The elemental mapping based on energy dispersive spectrometry (EDS) analysis evinced a uniform nitrogen distribution along the fiber cross-section (Figure 1d). The process of Ni^{2+} migration into the fibers was also traced, where Ni^{2+} gradually spread from the edge of fiber to its center with the increment of soaking time, and finally distributed uniformly along the fiber (Figure 1e, i–iv). Similar results were also observed for other metal ions (Fe^{2+}, Co^{2+}, Cu^{2+}, and Zn^{2+}, Figures S10–S13), verifying the efficient coordination of TPY units with transition metal ions. It should be noted that the saturation complexation time where corresponding metal ions distributed uniformly along the fiber is different for Ni^{2+} (around 90 min) compared to others (all around 60 min), due to the smallest coordination rate of Ni^{2+} with TPY.[35]

The formation of TPY-M(II) complexes is further supported via UV–vis absorption spectroscopy (Figure 2a). Only one intense absorption peak was observed at 287 nm for PETB raw samples attributed to the $\pi \rightarrow \pi^*$ transition of TPY ligands. After coordination with transition metal ions, an intense absorption peak emerged at around 350 nm, ascribed to the metal-to-ligand charge-transfer transition from TPY-M(II) complexes.[46−48] As a result, the PETB-M(II) samples presented different colors (Figure S14). In FTIR spectra (Figure 2b), the bending vibration of C=N from free TPY units (absorption peak at 1584 cm^{-1}) in PETB raw samples was diminished after the introduction of M(II) ions, while a new peak at 1601 cm^{-1} appeared, convincing the successful formation of TPY-M(II) complexes.[49,50]

The complexation of TPY units in PETB-38 with different M^{2+} was also traced with uniaxial stress–strain tests, with the curves for Ni^{2+} presented in Figure 3a, while others are in the

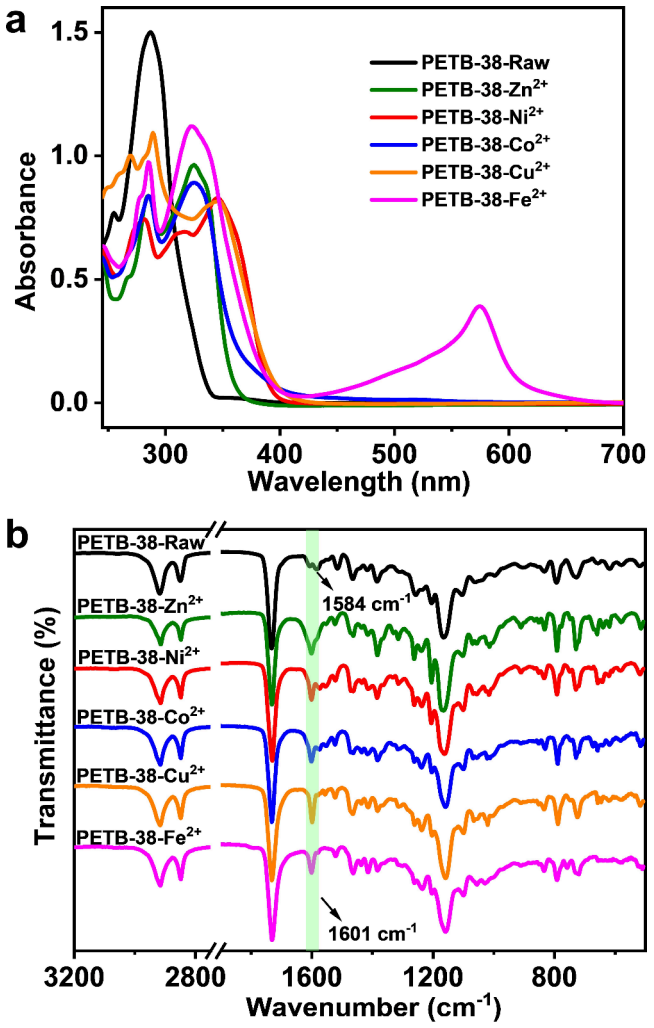

Figure 2. UV–vis absorption spectra (a) and ATR-FTIR spectra (b) of PETB copolyesters before and after complexation with different metal ions.

Supporting Information (Figures S15–S18 and summarized in Tables S2–S6). For complexation with Ni^{2+}, the Young's modulus, true stress at break, and toughness increased with soaking time and reached a plateau at about 90 min. This suggests most of the TPY units were complexed with Ni^{2+}, in accordance with the EDS results. Compared with the raw fibers, after soaking in Ni^{2+} solution for 90 min, the Young's modulus, true stress at break, and toughness of fibers increased from 180 to 431 MPa, 77.6 to 215 MPa, and 32.4 to 99.8 MJ m^{-3}, respectively. The mechanical properties were greatly strengthened without sacrificing their elongation at break, which is difficult to achieve in traditional chemical cross-linking systems. The strengthening and toughening mechanisms can be attributed to the introduction of metal–ligand SBs, which dissipate energy during breaking. For other transition metal ions, a similar trend is observed, but the complexation saturation time is around 60 min, consistent with the results from EDS mapping.

To study the effect of SB strength on mechanical property of toughened fibers, the uniaxial stress–strain curves of PETB-38 raw fiber and those PETB-38-M^{2+} with saturated coordination time are plotted in Figure 3b. The corresponding Young's modulus, true stress, and strain at break are summarized in Table 2. The Young's modulus increased dramatically after the

https://doi.org/10.1021/acs.macromol.3c02452
Macromolecules 2024, 57, 4054−4061

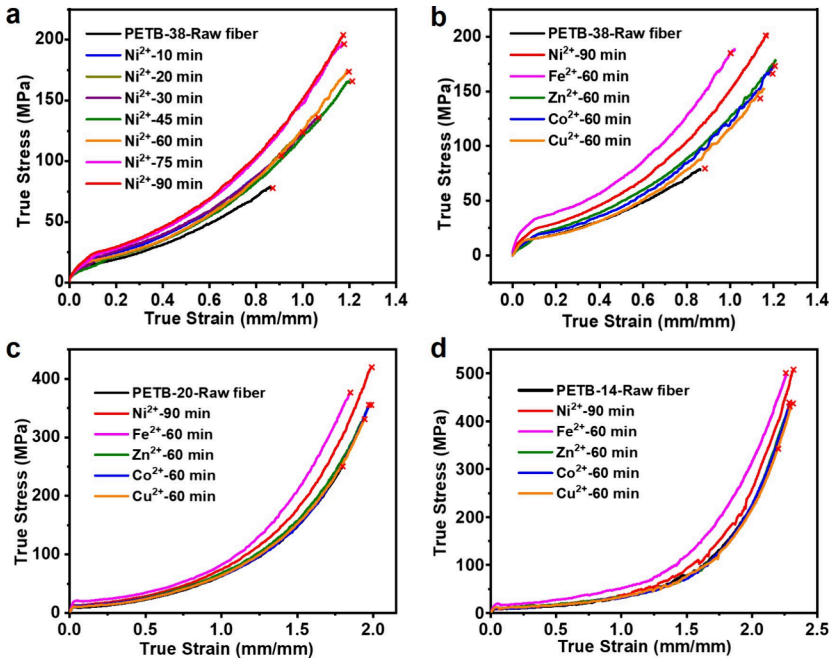

Figure 3. True stress−strain curves of PETB raw fibers and those metal-ion toughened fibers. (a) PETB-38 after coordination with Ni^{2+} for different times; PETB-38 (b), PETB-20 (c), and PETB-14 (d) after saturated coordination time with different metal ions.

Table 2. Uniaxial Tensile and Stress Relaxation Properties of PETB-38-M(II) Copolyester Fibers

sample	ΔH^a (kcal/mol)	Young's modulus (MPa)[b]	true stress at break (σ_T, MPa)[b]	true strain at break (ε_T)[b]	toughness (MJ m^{-3})[b]	$\tau_{1/2}$[c] at 50% strain (s)	$\tau_{1/2}$[c] at 100% strain (s)
raw fiber		180 ± 22	78 ± 17	0.86 ± 0.06	32.4 ± 6.3	3496	51
Fe^{2+}-60 min	−38.4	592 ± 18	189 ± 27	1.02 ± 0.06	86.7 ± 4.3	1370	220
Co^{2+}-60 min	−28.2	288 ± 37	173 ± 14	1.15 ± 0.06	82.1 ± 8.0	790	195
Ni^{2+}-90 min	−31.2	345 ± 15	202 ± 32	1.20 ± 0.20	96.0 ± 12.0	1436	280
Cu^{2+}-60 min	−33.8	274 ± 41	153 ± 22	1.15 ± 0.09	81.3 ± 12.3	330	68
Zn^{2+}-60 min	−28.4	257 ± 37	180 ± 24	1.21 ± 0.01	85.6 ± 5.4	1366	96

[a]The metal ligand binding enthalpies of $M(TPY)_2^{2+}$ tested in acetonitrile via isothermal titration calorimetry reported in ref 40. [b]Obtained from uniaxial tensile tests. [c]The characteristic relaxation time at $\sigma/\sigma_0 = 0.5$.

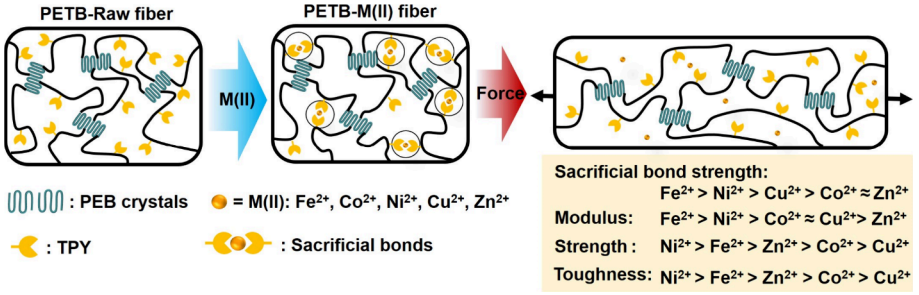

Figure 4. Schematic illustration of toughened fibers by the introduction of SBs.

formation of SBs, due to the increased cross-linking density among the elastomers.[51] Interestingly, Fe^{2+} provides the highest Young's modulus increment, while Zn^{2+} is the smallest. The trend for the order of Young's modulus increment roughly follows that of the coordination bond strength, i.e., $Fe^{2+} > Ni^{2+} > Co^{2+} \approx Cu^{2+} > Zn^{2+}$. For true stress at break (strength), however, Ni^{2+} affords the largest tensile strength enhancement while Fe^{2+} is the second, with the trend of $Ni^{2+} > Fe^{2+} > Zn^{2+} > Co^{2+} > Cu^{2+}$. When looking at the true strain at break, there is a slight increment after complexation, yet Fe^{2+} provides the smallest while others are similar. As a result, PETB-38-Ni^{2+} provides the highest toughness among the studied ions, with the order of $Ni^{2+} > Fe^{2+} > Zn^{2+} > Co^{2+} > Cu^{2+}$, similar to that of strength. These results indicate that when the SBs are too strong, they may not be broken before the breaking of other interactions (physical cross-links and/or covalent bonds); thus,

https://doi.org/10.1021/acs.macromol.3c02452
Macromolecules 2024, 57, 4054−4061

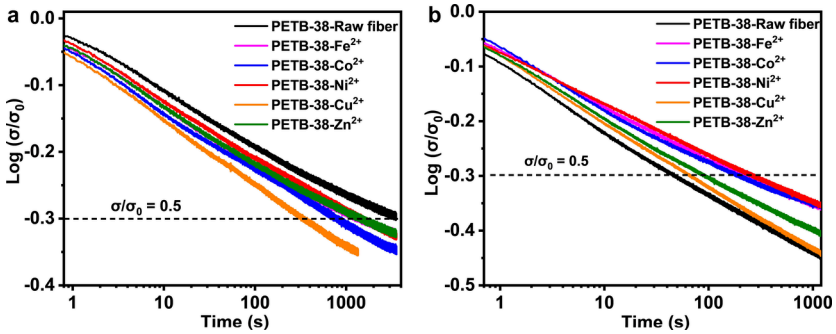

Figure 5. Stress relaxation curves for PETB-38 and toughened PETB-38-M(II) fibers at 50% (a) and 100% strain (b).

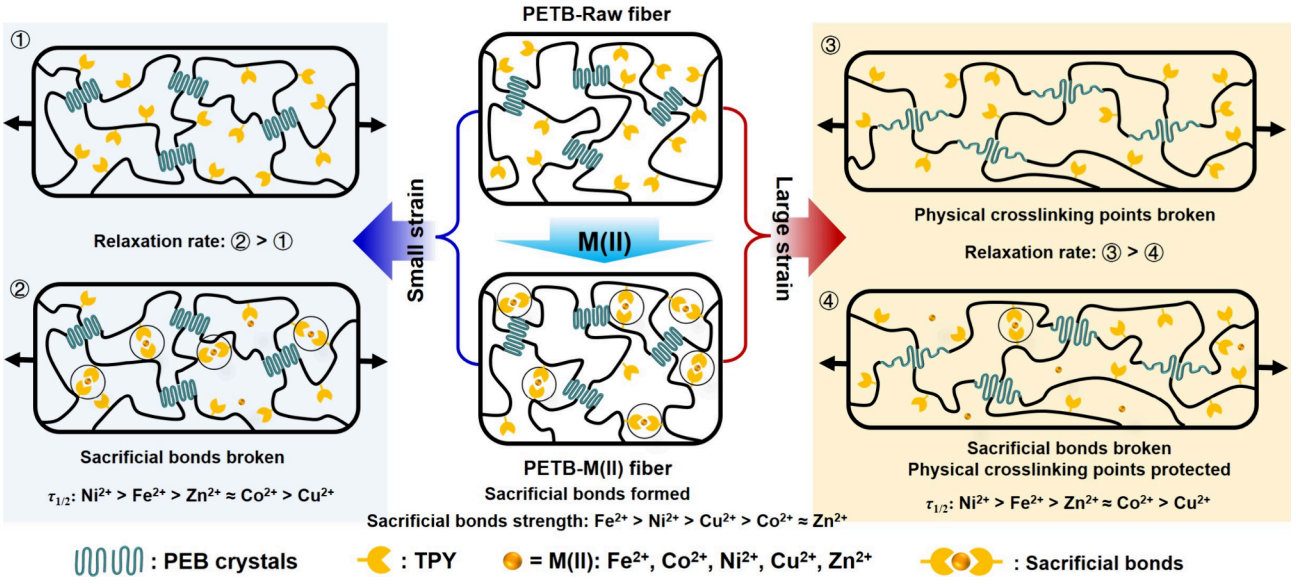

Figure 6. Schematic illustration of the stress relaxation of toughened fibers at small and large strains.

their "sacrificial" nature is hindered. As observed in Fe^{2+}, their strain at break is the smallest among all of the studied ions. Thus, the system with the strongest SBs may not afford the best strength, strain, and toughness enhancement. The toughening effect of different metal ions is illustrated in Figure 4.

For Cu^{2+}, which forms relatively strong coordination bonds with TPY, it shows the lowest strength and toughness enhancement. This can be attributed to its preferential monocoordination with TPY ($Cu(TPY)^{2+}$) when Cu^{2+} is in excess.[40] During the metal ion introduction process, Cu^{2+} migrated from the fiber outer layer to the core; thus, some of $Cu(TPY)_2{}^{2+}$ formed in sheath was converted to the monocoordination complex, reducing the supramolecular cross-linking density. This is supported by the Young's modulus decrement after the saturation complexation time (60 min).

To elucidate that the property difference is due to the introduction of coordination bonds but not the crystallinity change after complexation, all PETB-38 samples were characterized by DSC and WAXD (Figure S19 and Table S7). DSC results indicate the melting enthalpy for PEB segments decreased slightly after the formation of complexes. The peaks (21.65°, 24.02°, 30.01°, 36.23°, 40.51°, and 43.88°) observed from WAXD are the characteristic peaks for PEB crystals. After complexation with metal ions, the full width at half-maximum intensity (fwhm) was slightly increased, indicating that the PEB crystal size decreased slightly after the formation of coordination bonds. Since typically the strength and Young's modulus of a polymeric material increase with enhanced crystallinity, these results suggest that the improved mechanical properties come from the formation of SBs.

The stress−strain curves of copolyesters with less TPY content (PETB-20 and PETB-14) and their corresponding metal ion toughened fibers with saturated coordination time are presented in Figure 3c,d, with the results summarized in Tables S8 and S9. Similarly, the Young's modulus, strength, strain at break, and toughness increase after the introduction of metal ions. In addition, Fe^{2+} affords the highest Young's modulus but the lowest strain at break increment, while Ni^{2+} provides the highest strength and toughness enhancement. On the other hand, Cu^{2+} shows the lowest toughening effect with the smallest strength.

When compared to the three series of toughened fibers with the same metal ion, PETB-14-M^{2+} shows the largest strength, strain at break, and toughness. This can be attributed to the increased crystallinity of PEB in PETB raw fibers with TPY content decrement. In thermoplastic elastomers, the crystals act as the physically cross-linking points, leading to mechanical property enhancement.[52] Interestingly, PETB-20-M^{2+} samples roughly show the highest Young's modulus. This can be ascribed to the play of supramolecular cross-linking density together with the crystallinity of PETB. Increasing TPY

https://doi.org/10.1021/acs.macromol.3c02452
Macromolecules 2024, 57, 4054−4061

content will enhance the supramolecular cross-linking density that increases Young's modulus, but will reduce the crystallinity (physically cross-linking density) of PETB which decreases Young's modulus.

In addition, the above results indicate that the enhancement mechanism for Young's modulus is different from that for the strength, strain at break, and toughness. This is reasonable since the former is estimated at low strain (<10%), while the latters are measured at the maximum strain (typically >100% for elastomers).

To gain a deep insight into the dynamic mechanism in toughened fibers, stress relaxation experiments were carried out for PETB-38-M(II) samples, with the curves for 50 and 100% strain shown in Figure 5a,b, respectively. At 50% strain, the toughened fibers present faster relaxation rate compared with the raw fibers, presumably due to the breaking of coordination bonds to release inner stress. Among them, Cu^{2+} shows the fastest relaxation rate while Ni^{2+} the lowest. At 100% strain, the order is roughly the same, yet $\tau_{1/2}$ is much smaller, suggesting the polymer chains relaxed much faster at higher strains. The relaxation rate can be better represented by the characteristic stress relaxation time ($\tau_{1/2}$) listed in Table 2. It shows an order of $Ni^{2+} > Fe^{2+} > Zn^{2+} > Co^{2+} > Cu^{2+}$, which is roughly the same as in the strength order of toughened fibers.

At 50% strain, the PETB raw fiber shows a much slower relaxation rate compared to PETB-M^{2+} toughened fibers, while at 100% strain, it shows a faster relaxation rate with the smallest $\tau_{1/2}$. Both the breaking of coordination bonds and physically cross-linking points (crystals) can release the stress. For the raw polymers without coordination bonds, the physically cross-linking points retain at small strain but are destroyed at large strain as shown in Figure 6. By contrast, for toughened polymers, the coordination bonds break first to release the inner stress, thereby protecting some of the physically cross-linking points. At small strains, they relaxed faster than the raw polymer by the breaking of SBs. At large strains, due to the existence of the physically cross-linking points, they show a slower relaxation rate than the raw fibers. Our toughened system can be regarded as an elastomer with two kinds of SBs, where the breaking of weak SBs protects the stronger SBs. The schematic illustration of the mechanism is presented in Figure 6.

As the coordination bonds are easy to break under stress, the *in situ* tensile-FTIR experiments of toughened material were carried out (Figure S20). At different elongation ratio, the absorption peak at 1601 cm^{-1} ascribed to the metal−ligand coordination bonds does not show a significant change. This indicates that their dynamic exchanges (bond breaking and reformation) are quite fast and beyond the resolution of FTIR during stretching.

CONCLUSIONS

In summary, by the coordination of dangling TPY ligands with various transition metal ions, together with the PEB crystals as physically cross-linking points, elastomers with a double cross-linked network structure are constructed with tunable SBs and enhance mechanical properties. The metal−ligand complex with stronger coordination bond strength affords a toughened elastomer with higher Young's modulus, but when the coordination bonds are too strong, their sacrificial nature is weakened, and those property increments measured at high strain (strength, breaking strain, and toughness) are reduced. Stress relaxation experiments revealed that the relaxation rate becomes faster in the system with weaker coordination bonds, and the breaking of these SBs during stretching protects the physically cross-linking networks.

ASSOCIATED CONTENT

Supporting Information

The Supporting Information is available free of charge at https://pubs.acs.org/doi/10.1021/acs.macromol.3c02452.

Reagents, methods, experimental details, and additional characterization data including MALDI-TOF MS, ^1H NMR, GPC, DSC, FTIR, XRD, UV−vis, uniaxial tensile tests, SEM, EDS mapping, and so on (PDF)

AUTHOR INFORMATION

Corresponding Authors

Xiaohong Li − *Jiangsu Key Laboratory of Advanced Functional Polymer Design and Application, College of Chemistry, Chemical Engineering and Materials Science, Soochow University, Suzhou 215123, China;* orcid.org/0000-0003-3190-7214; Email: lxh83@suda.edu.cn

Yingfeng Tu − *Jiangsu Key Laboratory of Advanced Functional Polymer Design and Application, College of Chemistry, Chemical Engineering and Materials Science, Soochow University, Suzhou 215123, China;* orcid.org/0000-0001-6221-9145; Email: tuyingfeng@suda.edu.cn

Authors

Jie Chen − *Jiangsu Key Laboratory of Advanced Functional Polymer Design and Application, College of Chemistry, Chemical Engineering and Materials Science, Soochow University, Suzhou 215123, China*

Sheng Wang − *Jiangsu Key Laboratory of Advanced Functional Polymer Design and Application, College of Chemistry, Chemical Engineering and Materials Science, Soochow University, Suzhou 215123, China*

Jie Huan − *Jiangsu Key Laboratory of Advanced Functional Polymer Design and Application, College of Chemistry, Chemical Engineering and Materials Science, Soochow University, Suzhou 215123, China*

Zhikai Li − *College of Chemistry and Environmental Engineering, Shenzhen University, Shenzhen, Guangdong 518060, China;* orcid.org/0000-0002-9781-2747

Xiaoming Yang − *Jiangsu Key Laboratory of Advanced Functional Polymer Design and Application, College of Chemistry, Chemical Engineering and Materials Science, Soochow University, Suzhou 215123, China;* orcid.org/0000-0002-5324-7416

Complete contact information is available at: https://pubs.acs.org/10.1021/acs.macromol.3c02452

Notes

The authors declare no competing financial interest.

ACKNOWLEDGMENTS

The financial support from the National Natural Science Foundation of China (Grant Nos. 22071167 and 22231008), the Natural Science Foundation of Jiangsu Higher Education Institutions of China (22KJA150005), and a project funded by the Priority Academic Program Development of Jiangsu Higher Education Institutions is gratefully acknowledged.

REFERENCES

(1) Harrington, M. J.; Masic, A.; Holten-Andersen, N.; Waite, J. H.; Fratzl, P. Iron-Clad Fibers: A Metal-Based Biological Strategy for Hard Flexible Coatings. *Science* **2010**, *328*, 216−220.

(2) Zechel, S.; Hager, M. D.; Priemel, T.; Harrington, M. J. Healing through Histidine: Bioinspired Pathways to Self-Healing Polymers via Imidazole-Metal Coordination. *Biomimetics* **2019**, *4*, 20−40.

(3) Schmitt, C. N.; Politi, Y.; Reinecke, A.; Harrington, M. J. Role of Sacrificial Protein-Metal Bond Exchange in Mussel Byssal Thread Self-Healing. *Biomacromolecules* **2015**, *16*, 2852−2861.

(4) Zhang, J.; Huang, C.; Zhu, Y.; Huang, G.; Wu, J. Toughening Polyisoprene Rubber with Sacrificial Bonds: The Interplay between Molecular Mobility, Energy Dissipation and Strain-Induced Crystallization. *Polymer* **2021**, *231*, No. 124114.

(5) Zhou, X.; Guo, B.; Zhang, L.; Hu, G. H. Progress in Bio-Inspired Sacrificial Bonds in Artificial Polymeric Materials. *Chem. Soc. Rev.* **2017**, *46*, 6301−6329.

(6) Fantner, G. E.; Oroudjev, E.; Schitter, G.; Golde, L. S.; Thurner, P.; Finch, M. M.; Turner, P.; Gutsmann, T.; Morse, D. E.; Hansma, H.; et al. Sacrificial Bonds and Hidden Length: Unraveling Molecular Mesostructures in Tough Materials. *Biophys. J.* **2006**, *90*, 1411−1418.

(7) Huang, Y.; Li, J.; Qi, M.; Si, G.; Tan, C. In Situ Modification to Reinforce Isoprene Rubber by Sacrificial Bonds. *ACS Appl. Polym. Mater.* **2023**, *5*, 4080−4087.

(8) Xu, J.; Wang, X.; Ruan, H.; Zhang, X.; Zhang, Y.; Yang, Z.; Wang, Q.; Wang, T. Recent Advances in High-Strength and High-Toughness Polyurethanes Based on Supramolecular Interactions. *Polym. Chem.* **2022**, *13*, 2420−2441.

(9) Yao, Y.; Liu, B.; Xu, Z.; Yang, J.; Liu, W. An Unparalleled H-Bonding and Ion-Bonding Crosslinked Waterborne Polyurethane with Super Toughness and Unprecedented Fracture Energy. *Mater. Horiz.* **2021**, *8*, 2742−2749.

(10) Li, Z.; Zhu, Y. L.; Niu, W.; Yang, X.; Jiang, Z.; Lu, Z. Y.; Liu, X.; Sun, J. Healable and Recyclable Elastomers with Record-High Mechanical Robustness, Unprecedented Crack Tolerance, and Superhigh Elastic Restorability. *Adv. Mater.* **2021**, *33*, No. 2101498.

(11) Li, C. H.; Wang, C.; Keplinger, C.; Zuo, J. L.; Jin, L.; Sun, Y.; Zheng, P.; Cao, Y.; Lissel, F.; Linder, C. A Highly Stretchable Autonomous Self-Healing Elastomer. *Nat. Chem.* **2016**, *8*, 618−624.

(12) Shao, J.; Dong, X.; Wang, D. Stretchable Self-Healing Plastic Polyurethane with Super-High Modulus by Local Phase-Lock Strategy. *Macromol. Rapid Commun.* **2022**, *44*, No. e2200299.

(13) Cai, Y.; Wang, Y.; Long, L.; Zhou, S.; Yan, L.; Zhang, J.; Zou, H. Fabrication of Highly Thermally Resistant and Self-Healing Polysiloxane Elastomers by Constructing Covalent and Reversible Networks. *Macromol. Rapid Commun.* **2023**, *44*, No. e300191.

(14) Zhang, H.; He, J.; Qu, J. Metal-Coordinated Amino Acid Hydrogels with Ultra-Stretchability, Adhesion, and Self-Healing Properties for Wound Healing. *Eur. Polym. J.* **2022**, *179*, No. 111548.

(15) Ju, H.; Zhu, Q. L.; Zuo, M.; Liang, S.; Du, M.; Zheng, Q.; Wu, Z. L. Toughening Hydrogels by Forming Robust Hydrazide-Transition Metal Coordination Complexes. *Chem.—Eur. J.* **2023**, *29*, No. e202300969.

(16) Huang, Y. S.; Zhou, Y.; Zeng, X.; Zhang, D.; Wu, S. Reversible Crosslinking of Commodity Polymers via Photocontrolled Metal-Ligand Coordination for High-Performance and Recyclable Thermoset Plastics. *Adv. Mater.* **2023**, *35*, No. e2305517.

(17) Lin, P.; Ma, S.; Wang, X.; Zhou, F. Molecularly Engineered Dual-Crosslinked Hydrogel with Ultrahigh Mechanical Strength, Toughness, and Good Self-Recovery. *Adv. Mater.* **2015**, *27*, 2054−2059.

(18) Yang, C. H.; Wang, M. X.; Haider, H.; Yang, J. H.; Sun, J. Y.; Chen, Y. M.; Zhou, J.; Suo, Z. Strengthening Alginate/Polyacrylamide Hydrogels Using Various Multivalent Cations. *ACS Appl. Mater. Interfaces* **2013**, *5*, 10418−10422.

(19) Bao, J.; Li, X.; Wang, J.; Cong, Y.; Zhou, J.; Zhang, X.; Chen, W. Crystallization, Morphology and Mechanical Property Enhancement of Block Copolymer-Based Metallosupramolecular Polymers by Incorporating Metal Coordinating Ligand into Poly(L-lactic acid) Block. *Polymer* **2022**, *256*, No. 125191.

(20) Jiang, F.; Fang, C.; Zhang, J.; Wang, W. T.; Wang, Z. G. Triblock Copolymer Elastomers with Enhanced Mechanical Properties Synthesized by RAFT Polymerization and Subsequent Quaternization through Incorporation of a Comonomer with Imidazole Groups of about 2.0 Mass Percentage. *Macromolecules* **2017**, *50*, 6218−6226.

(21) Fullenkamp, D. E.; He, L.; Barrett, D. G.; Burghardt, W. R.; Messersmith, P. B. Mussel-Inspired Histidine-Based Transient Network Metal Coordination Hydrogels. *Macromolecules* **2013**, *46*, 1167−1174.

(22) Li, C.; Tan, J.; Guan, Z.; Zhang, Q. A Three-Armed Polymer with Tunable Self-Assembly and Self-Healing Properties Based on Benzene-1,3,5-tricarboxamide and Metal-Ligand Interactions. *Macromol. Rapid Commun.* **2019**, *40*, No. e1800909.

(23) Tang, Z. H.; Huang, J.; Guo, B. C.; Zhang, L. Q.; Liu, F. Bioinspired Engineering of Sacrificial Metal−Ligand Bonds into Elastomers with Supramechanical Performance and Adaptive Recovery. *Macromolecules* **2016**, *49*, 1781−1789.

(24) Wang, X.; Zhan, S.; Lu, Z.; Li, J.; Yang, X.; Qiao, Y.; Men, Y.; Sun, J. Healable, Recyclable, and Mechanically Tough Polyurethane Elastomers with Exceptional Damage Tolerance. *Adv. Mater.* **2020**, *32*, No. e2005759.

(25) Li, Z.; Wang, J.; Li, X.; Wang, Y.; Fan, L. J.; Yang, S.; Guo, M.; Li, X.; Tu, Y. Supramolecular and Physically Double-Cross-Linked Network Strategy toward Strong and Tough Elastic Fibers. *ACS Macro Lett.* **2020**, *9*, 1655−1661.

(26) Liu, H.; Lin, R.; Huang, Z.; Yin, X.; Lin, X.; Lin, W.; Li, Y.; Gu, Y.; Yi, G. Modified Ethylene/α-Octene Copolymer Elastomer Composites with Sacrificial Bonds Crosslinking Networks and Their Reinforced Mechanical Performance. *Polym. Eng. Sci.* **2023**, *63*, 921−931.

(27) Fan, J.; Zhou, X.; Chen, Y. Multiple Hierarchical Dynamic Interactions Enabled a Robust, Stretchable and Room Temperature Self-Healing Elastomer. *Polym. Chem.* **2023**, *14*, 2117−2125.

(28) Mareliati, M.; Tadiello, L.; Guerra, S.; Giannini, L.; Schrettl, S.; Weder, C. Metal−Ligand Complexes as Dynamic Sacrificial Bonds in Elastic Polymers. *Macromolecules* **2022**, *55*, 5164−5175.

(29) Hu, R.; Zhao, S.; Chen, F.; Shangguan, Y.; Zheng, Q. Effect of Sacrificial Bond on Molecular Dynamics and Rheological Behavior of Hybrid Butadiene-Styrene-Vinylpyridine Rubber Vulcanizates with Reversible Sacrificial Network. *J. Polym. Sci.* **2022**, *60*, E1−E12.

(30) Cai, Y.; Li, H.; Li, C.; Tan, J.; Zhang, Q. A Strategy of Thiolactone Chemistry to Construct Strong and Tough Self-Healing Supramolecular Polyurethane Elastomers via Hierarchical Hydrogen Bonds and Coordination Bonds. *Ind. Eng. Chem. Res.* **2023**, *62*, 6416−6424.

(31) Williams, K. A.; Boydston, A. J.; Bielawski, C. W. Main-Chain Organometallic Polymers: Synthetic Strategies, Applications, and Perspectives. *Chem. Soc. Rev.* **2007**, *36*, 729−744.

(32) Chi, Z.; Ma, C.; He, Z.; Ma, Z.; Chen, X.; Huang, Z. A Supramolecular Hydrogel Based on Copolymers of Acrylic Acid and Maleic Anhydride Derivatives with Terpyridine Motifs. *Polymers* **2022**, *14*, 2857.

(33) Meurer, J.; Bätz, T.; Hniopek, J.; Bernt, C.; Zechel, S.; Schmitt, M.; Popp, J.; Hager, M. D.; Schubert, U. S. Application of Orthogonal Metal−Ligand Interactions for the Synthesis of Interpenetrating Metallopolymer Networks Featuring Shape-Memory and Self-Healing Abilities. *J. Mater. Chem. A* **2022**, *10*, 25106−25117.

(34) Han, T.-Y.; Lin, C.-H.; Lin, Y.-S.; Yeh, C.-M.; Chen, Y.-A.; Li, H.-Y.; Xiao, Y.-T.; Chang, J.-W.; Su, A.-C.; Jeng, U. S.; et al. Autonomously Self-Healing and Ultrafast Highly-Stretching Recoverable Polymer through Trans-Octahedral Metal-Ligand Coordination for Skin-Inspired Tactile Sensing. *Chem. Eng. J.* **2022**, *438*, No. 135592.

(35) Holyer, R. H.; Hubbard, C. D.; Kettle, S. F. A.; Wilkins, R. G. The Kinetics of Replacement Reactions of Complexes of the

https://doi.org/10.1021/acs.macromol.3c02452
Macromolecules 2024, 57, 4054−4061

Transition Metals with 2,2′,2″-Terpyridine. *Inorg. Chem.* **1966**, *5*, 622−625.
(36) Li, J.; Wang, S.; Lu, H.; Tu, Y.; Wan, X.; Li, X.; Tu, Y.; Li, C. Y. Helical Crystals in Aliphatic Copolyesters: From Chiral Amplification to Mechanical Property Enhancement. *ACS Macro Lett.* **2023**, *12*, 369−375.
(37) Li, J.; Wang, S.; Lu, H.; Lan, Y.; Li, X.; Tu, Y. Chemical Recycling of Poly(ethylene furanoate) into Value-Added Poly(ethylene-*co*-isosorbide furanoate). *Chin. J. Polym. Sci.* **2023**, *41*, 1533−1542.
(38) Tu, Y. F. Cascade Polymerization. *Acta Polym. Sin.* **2019**, *50*, 1145−1155.
(39) Wan, X. T.; Jiang, J.; Tu, Y. Y.; Xu, S. Y.; Li, J.; Lu, H. J.; Li, Z. K.; Xiong, L. H.; Li, X. H.; Zhao, Y. L. A Cascade Strategy towards the Direct Synthesis of Green Polyesters with Versatile Functional Groups. *Polym. Chem.* **2021**, *12*, 6022−6029.
(40) Dobrawa, R.; Ballester, P.; Saha-Möller, C. R.; Würthner, F. Thermodynamics of 2,2′:6′,2″-Terpyridine-metal Ion Complexation. In *Metal-Containing and Metallosupramolecular Polymers and Materials*; American Chemical Society, 2006; p 57.
(41) Hanan, G. S.; Wang, J. H. A Facile Route to Sterically Hindered and Non-Hindered 4′-Aryl-2,2′:6′,2″-Terpyridines. *Synlett* **2005**, *2005*, 1251−1254.
(42) Wild, A.; Winter, A.; Schlutter, F.; Schubert, U. S. Advances in the Field of pi-Conjugated 2,2′:6′,2″-Terpyridines. *Chem. Soc. Rev.* **2011**, *40*, 1459−1511.
(43) Fernandez, J.; Amestoy, H.; Sardon, H.; Aguirre, M.; Varga, A. L.; Sarasua, J. R. Effect of Molecular Weight on the Physical Properties of Poly(ethylene brassylate) Homopolymers. *J. Mech. Behav. Biomed. Mater.* **2016**, *64*, 209−219.
(44) Marxsen, S. F.; Song, D.; Zhang, X.; Flores, I.; Fernández, J.; Sarasua, J. R.; Müller, A. J.; Alamo, R. G. Crystallization Rate Minima of Poly(ethylene brassylate) at Temperatures Transitioning between Quantized Crystal Thicknesses. *Macromolecules* **2022**, *55*, 3958−3973.
(45) Wang, Z.; Song, M.; Li, X.; Chen, J.; Liang, T.; Chen, X.; Yan, Y. Copolymerization-Regulated Hydrogen Bonds: A New Routine for High-Strength Copolyamide 6/66 Fibers. *Polymers* **2022**, *14*, 3517−3530.
(46) Wu, D.; Shao, T.; Men, J.; Chen, X.; Gao, G. Superaromatic Terpyridines Based on Corannulene Responsive to Metal Ions. *Dalton Trans.* **2014**, *43*, 1753−1761.
(47) Hofmeier, H.; Schubert, U. S. Supramolecular Branching and Crosslinking of Terpyridine-Modified Copolymers: Complexation and Decomplexation Studies in Diluted Solution. *Macromol. Chem. Phys.* **2003**, *204*, 1391−1397.
(48) Beck, J. B.; Ineman, J. M.; Rowan, S. J. Metal/Ligand-Induced Formation of Metallo-Supramolecular Polymers. *Macromolecules* **2005**, *38*, 5060−5068.
(49) Meurer, J.; Bätz, T.; Hniopek, J.; Zechel, S.; Schmitt, M.; Popp, J.; Hager, M. D.; Schubert, U. S. Dual Crosslinked Metallopolymers Using Orthogonal Metal Complexes as Rewritable Shape-Memory Polymers. *J. Mater. Chem. A* **2021**, *9*, 15051−15058.
(50) Wang, Z.; Xie, C.; Yu, C.; Fei, G.; Wang, Z.; Xia, H. A Facile Strategy for Self-Healing Polyurethanes Containing Multiple Metal-Ligand Bonds. *Macromol. Rapid Commun.* **2018**, *39*, No. e1700678.
(51) Liu, Y.; Tang, Z.; Wang, D.; Wu, S.; Guo, B. Biomimetic Design of Elastomeric Vitrimers with Unparalleled Mechanical Properties, Improved Creep Resistance and Retained Malleability by Metal−Ligand Coordination. *J. Mater. Chem. A* **2019**, *7*, 26867−26876.
(52) Tran, H.; Feig, V. R.; Liu, K.; Zheng, Y.; Bao, Z. N. Polymer Chemistries Underpinning Materials for Skin-Inspired Electronics. *Macromolecules* **2019**, *52*, 3965−3974.

https://doi.org/10.1021/acs.macromol.3c02452
Macromolecules 2024, 57, 4054−4061